A Complex Window-Based *Joint-Chirp-rate-Time-Frequency Transform* for BBH Merger Signal Detection using Spectrograms

Xiyuan Li[1], Martin Houde[1], Jignesh Mohanty[2], Sree Ram Valluri[1,3]

(Supervisor) (Supervisor)

[1]Department of Physics and Astronomy, University of Western Ontario, Canada

[2] Indian Institute of Technology Kanpur, India

[3]Mathematics, Kings University College, University of Western Ontario, Canada

Motivation

- Machine Learning (ML) algorithms have transformed the methods of data analysis, image pattern recognition, and math modeling.
- Artificial Neural Networks (ANNs) are among the most talked about techniques in the ML family with a wide range of applications.
  - Applications of ANNs

Self-driving Cars*

*Side-by-side camera view and ANN annotated LIDAR data (Waymo)

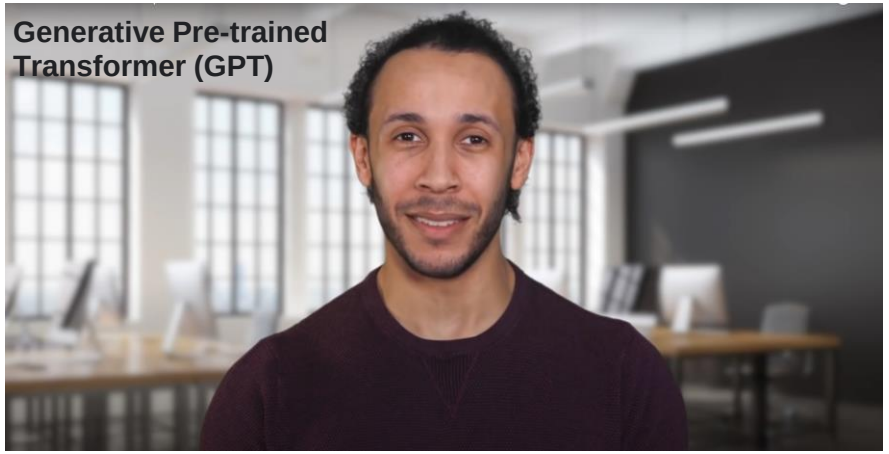

Natural Language Processing^

^AI chat robot with facial expressions, movements, and voice generated using GPT-3 (OpenAI)

What can ANNs do to accelerate Gravitational Wave (GW) research?

Motivation

- Active research areas:
  - Detector transient noise (glitch) classification.
  - Real-time Binary Black Hole (BBH) Binary Neutron Star (BNS) merger event detection.
  - BBH/BNS merger event forecasting.

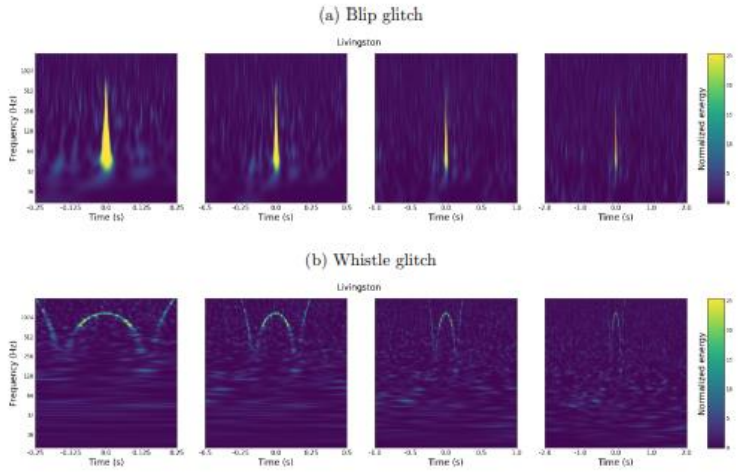

Glitch Classification*

***Spectrograms** of two types of glitches (Gravity Spy)

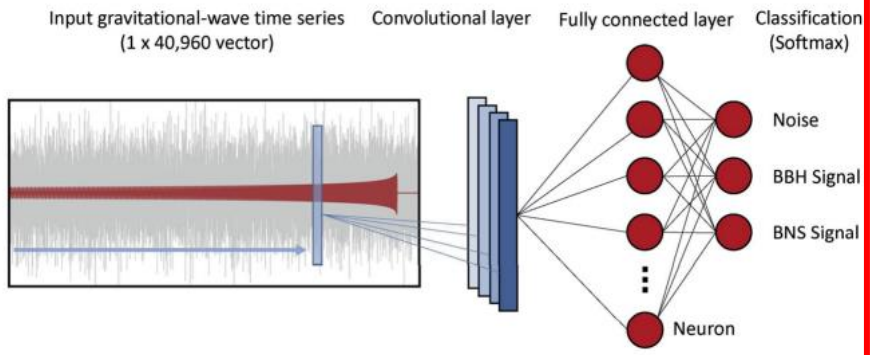

BBH/BNS Merger Detection^

^ Convolutional Neural Network (CNN) in merger event detection, classification. (Plamen G. Krastev)

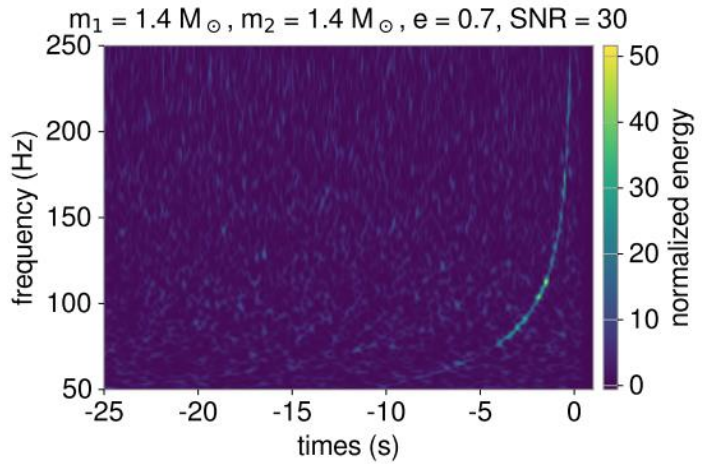

BBH/BNS Merger Forecasting◦

◦ **Spectrogram** of a simulated BNS merger signal (W. Wei and et al.)

M. Zevin and et al., "Gravity spy: integrating advanced ligo detector characterization, machine learning, and citizen science," Classical and Quantum Gravity, vol. 34, no. 6, p. 064003, 2017

Krastev, P. G. (2020). Real-time detection of gravitational waves from binary neutron stars using Artificial Neural Networks. *Physics Letters B*, *803*, 135330.

W. Wei and et al., "Deep learning with quantized neural networks for gravitational-wave forecasting of eccentric compact binary coalescence," The Astrophysical Journal, vol. 919, no. 2, p. 82, 2021

Objective

- Design a transform method that produces **chirp-rate enhanced spectrograms** to improve spectrogram classification networks' performance in **low signal-to-noise ratio** BBH, BNS merger signal detection and forecasting.

BBH BNS Merger GW Waveform

Our proposed method targets a specific type of GW signal produced by two merging compact objects:

- The energy of a binary merger system is lost in the form of radiating GW.
- This process causes the distance between the objects to decrease and the angular speed to increase, thus causing increasingly stronger GW emissions and higher angular frequencies.

Chirp signal: ~ changing frequency

BBH Merger Process and Waveform

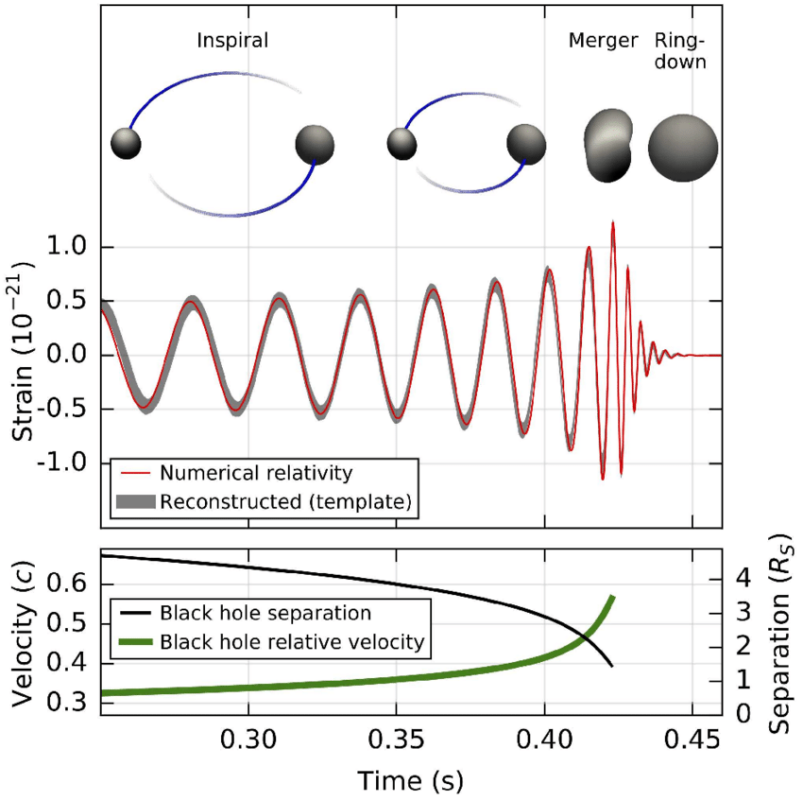

Francisco R. Villatoro (2018)

Current Detection Techniques

Technique 1: **Templated Search** – Matched Filtering

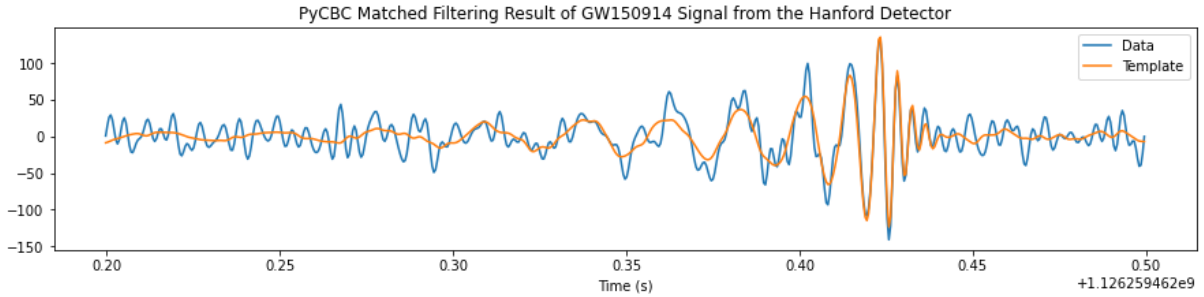

Hanford detector signal of BBH merger event GW150914 (September 14 2015, 09:50:45 UTC) plotted against the matched waveform template in PyCBC.

It compares the input signal to a set of signals in the template bank where numerically generated signals are stored at and the best match is determined following a series of vetoing algorithms.

Technique 2: **Non-templated Search** – Burst Search

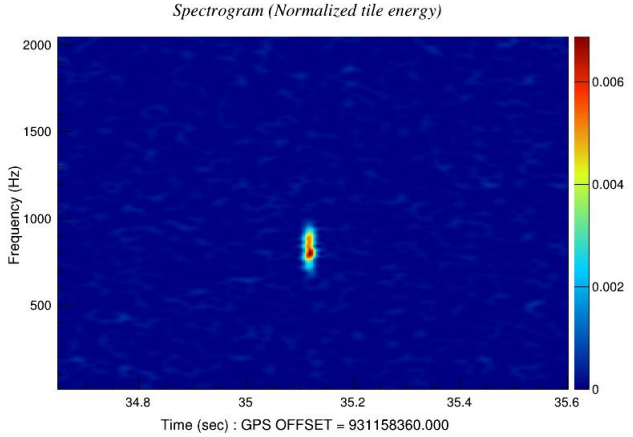

The spectrogram of an unknown event recorded by the Livingston detector at GPS time 931158360 (July 8 2009, 07:05:45 UTC), generated by the coherence waveBurst pipeline.

This search algorithm looks at chirp-like signals as potential mergers and flags them for further verification

Existing Spectrogram Generation Methods

- Short-time Fourier Transform (STFT)
- Gabor Transform (GT)
- Constant Q Transform (CQT)
- S (Stockwell) Transform (ST)
- …

- All use the Fourier transform as the foundation.
- Only decompose the relationship between time and frequency.
- The defining characteristic of a BBH merger signal, **the chirp**, is abandoned.

Constant Q Transform of GW 150914

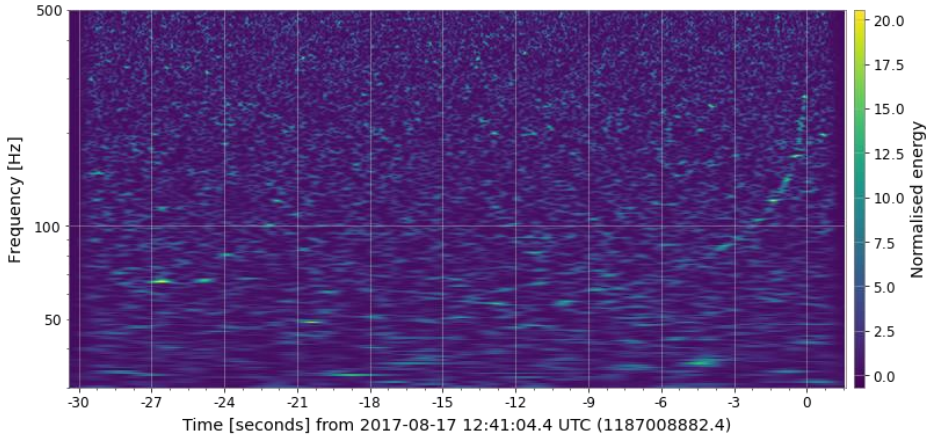

S Transform of a simulated BBH merger

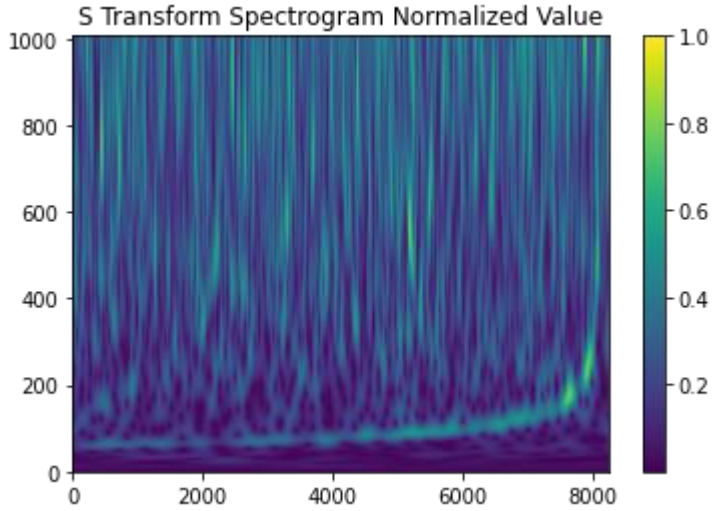

Simulated merger m1 = m2 =, normalized amplitude 1, injected to Gaussian noise of amplitude 10.

Obtaining the Chirp-rate Information

Fourier Transform (FT)

$$X(\Omega) = \int_{-\infty}^{\infty} x(t) e^{-i2\pi\Omega t} dt,$$

Linear Chirp Transform (LCT)

$$X(\Omega, \gamma) = \int_{-\infty}^{\infty} x(t) e^{-i2\pi(\Omega t + \gamma t^2)} dt.$$

O, A, Alkaishriwo & L.F. Chaparro (2012)

Matching the input signal x(t) to a **constant frequency** signal model: $e^{-\mathrm{i}2\pi\Omega t}$.

Matching the input signal x(t) to a **linear chirp** signal model: $e^{-\mathrm{i}2\pi(\Omega t+\gamma t^2)}$.

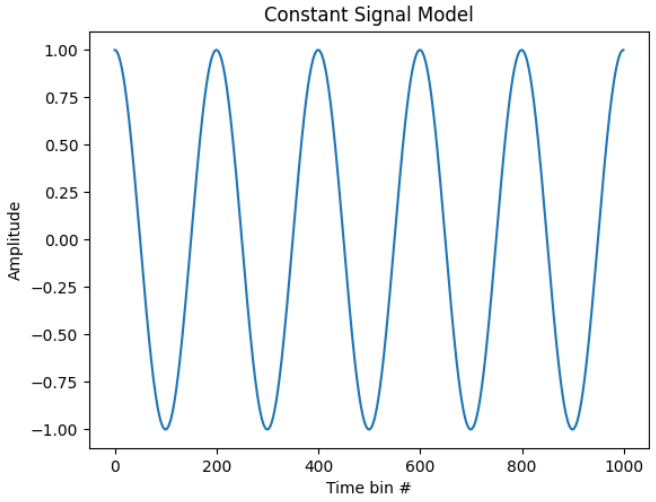

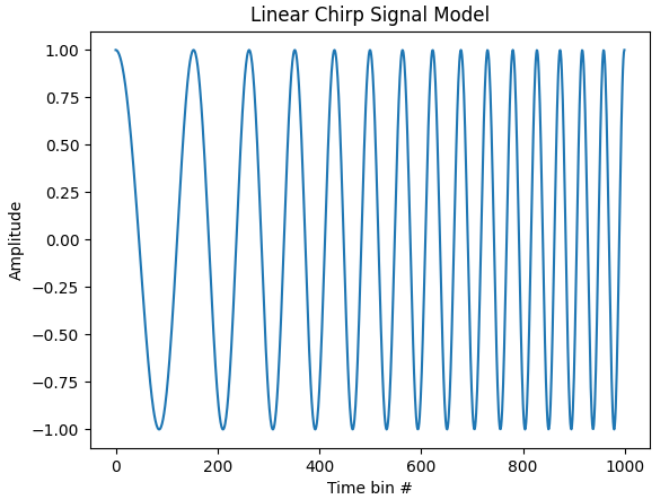

Obtaining the Chirp-rate Information

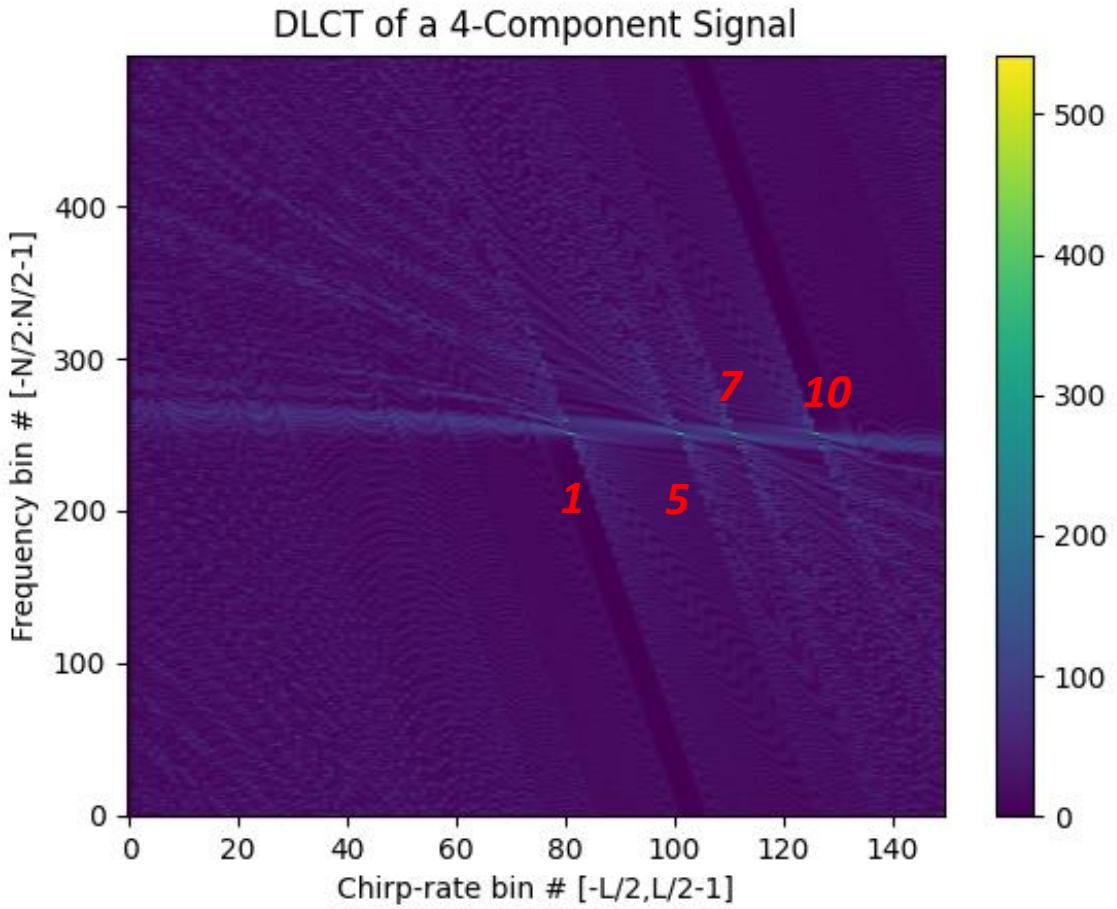

Discrete Linear Chirp Transform (DLCT) of a 4-component linear chirp signal.

Linear Chirp Transform (LCT)

$$X(\Omega,\gamma)=\int_{-\infty}^{\infty}x(t)e^{-i2\pi(\Omega t+\gamma t^2)}dt.$$

O, A, Alkaishriwo & L.F. Chaparro (2012)

$$x_{4-component}(t)=e^{j2\pi t^2}_{\mathbf{1}}+e^{j2\pi 5t^2}_{\mathbf{5}}+e^{j2\pi 7t^2}_{\mathbf{7}}+e^{j2\pi 10t^2}_{\mathbf{10}}$$

One can obtain the chirp rate and starting frequency of each chirp signal by further processing the Linear Chirp Transform frequency-chirp-rate diagram.

The Joint-Chirp-Rate-Time-Frequency Transform (JCTFT)

$$H_J(\gamma,\tau,\Omega)=\int_{-\infty}^{\infty} h(t)g_c(\gamma,t-\tau,\Omega)e^{-i2\pi\Omega t}dt,$$

$\gamma = 0$ → Short-Time Fourier Transform

$$g_c(\gamma,t-\tau,\Omega)=\frac{|\Omega_0+\mu\Omega|}{\sqrt{2\pi}}\frac{1+\frac{t-\tau}{|t-\tau|}}{2}e^{-(t-\tau)^2[\frac{(\Omega_0+\mu\Omega)^2}{2}+i2\pi\gamma]},$$

$\gamma = 0$ → Gaussian Window

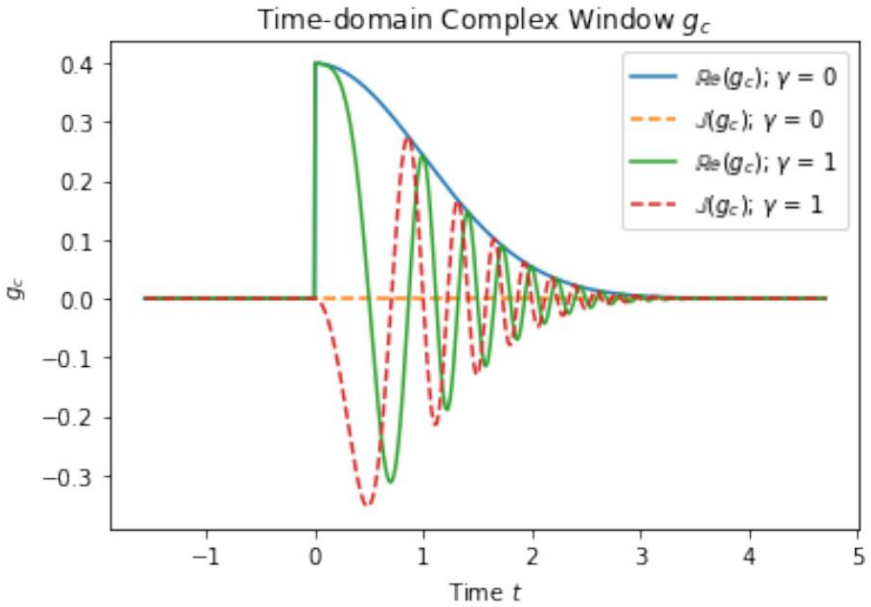

A 2D representation by taking an orthogonal projection of the JCTFT along the chirp rate axis:

$$S_J(\Omega,\tau)=\int_{-L}^{L} H_J(\gamma,\tau,\Omega)d\gamma,$$

An Alternative Definition using the Convolution Theorem

$$H_J(\gamma,\tau,\Omega) = \mathcal{F}\{f(t)g_c(t-\tau,\gamma,\Omega)\}$$
$$= \mathcal{F}\{f(t)\} * \mathcal{F}\{g_c(t-\tau,\gamma,\Omega)\}$$
$$= \mathcal{F}\{f(t)\} * \mathcal{F}\{g_c(t,\gamma,\Omega)\}e^{-i2\pi\Omega\tau},$$

an alternative frequency domain representation of the JCTFT is

$$H_J(\gamma,\tau,\Omega) = \int_{-\infty}^{\infty} H(\Omega+\alpha)G_c(\gamma,\Omega,\alpha)e^{i2\pi\alpha\tau}d\alpha,$$

and Gc is the Fourier transform of the complex linear chirp window function $g_c(t)$ with a dummy frequency variable α due to the convolution:

$$G_c(\gamma,\Omega,\alpha) = \frac{|\Omega_0+\mu\Omega|}{\sqrt{2\pi}}\{e^{-\pi^2\alpha^2/z}(\frac{1}{2}\sqrt{\frac{\pi}{z}}[1-erf(\frac{i\pi\alpha}{\sqrt{z}})])\},$$

where $z = a+ib$, $a = \frac{(\Omega_0+\mu\Omega)^2}{2}$, and $b = 2\pi\gamma$.

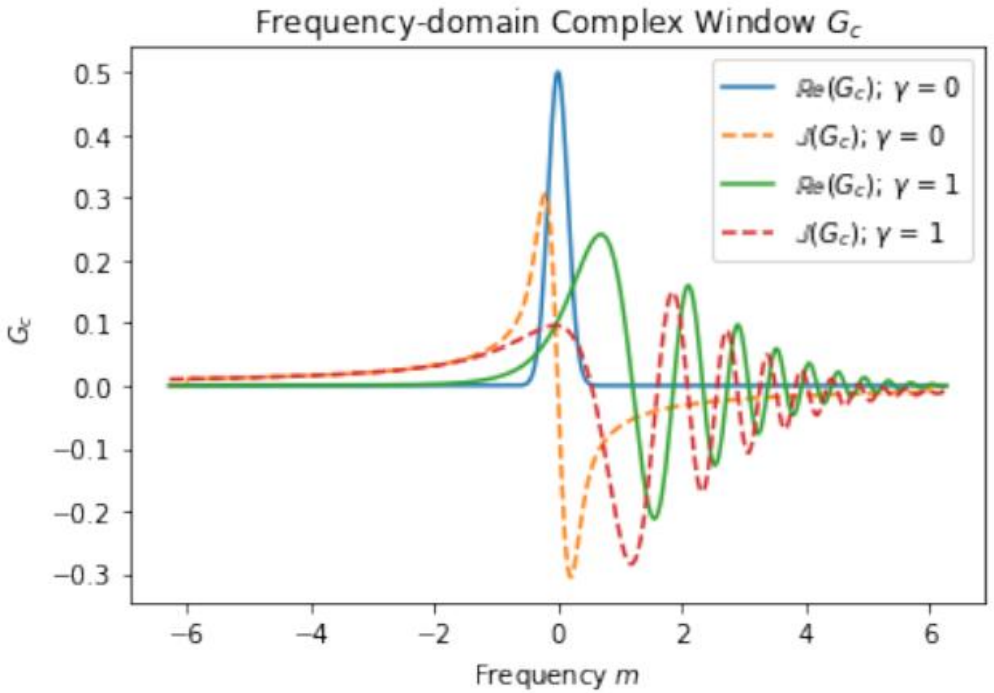

JCTFT vs. Q-Transform

$$H_J(\gamma,\tau,\Omega) = \int_{-\infty}^{\infty} H(\Omega+\alpha)G_c(\gamma,\Omega,\alpha)e^{i2\pi\alpha\tau}d\alpha,$$

$$S_J(\Omega,\tau) = \int_{-L}^{L} H_J(\gamma,\tau,\Omega)d\gamma,$$

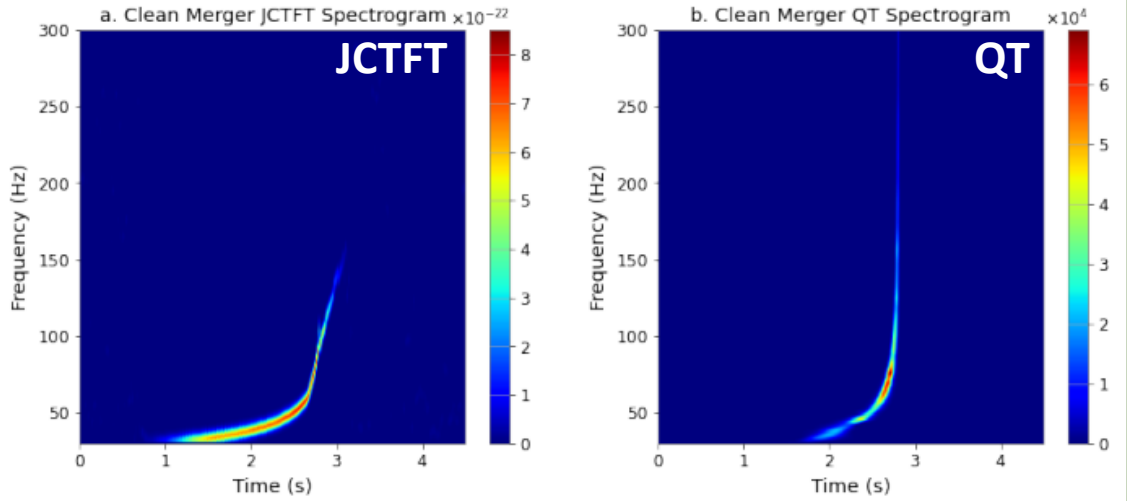

- ***Clean Merger***

Test signal: ***Merger**: SEOBNR-Phenom Model*
Starting Freq: 30 Hz ; Masses: 15 Solar, 10 Solar

***Noise**: aLIGO 0-detuned-Higher-Power*

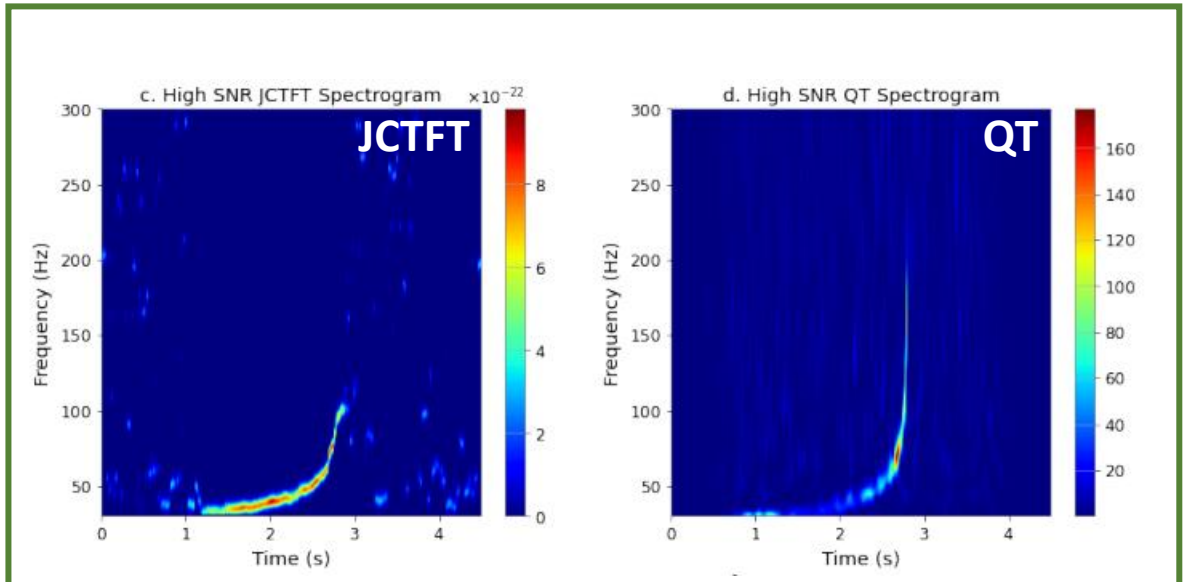

- ***Noisy Merger SNR 29.9***

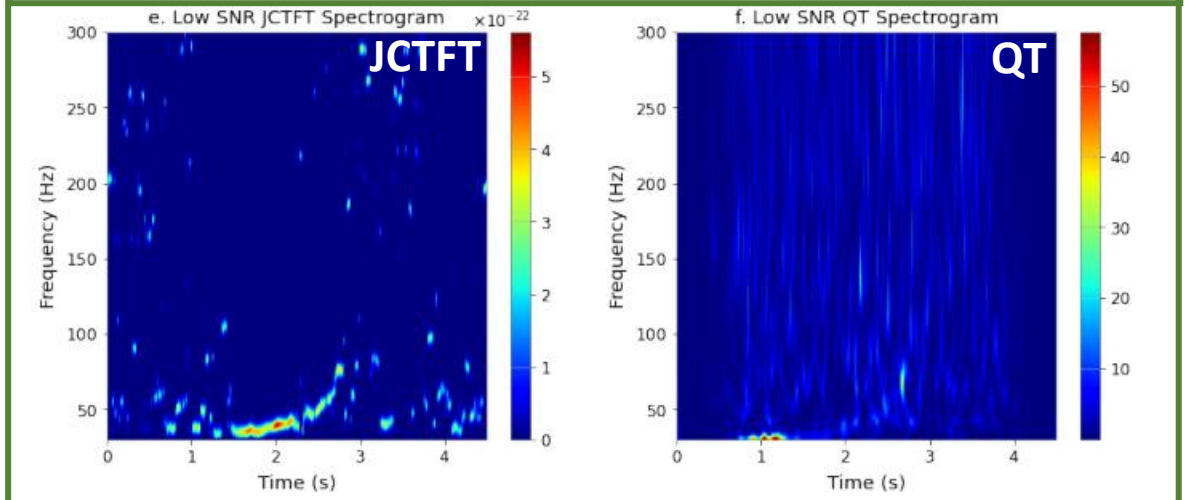

- ***Noisy Merger SNR 10.4***

Classification Accuracy using **Inception V3** Network

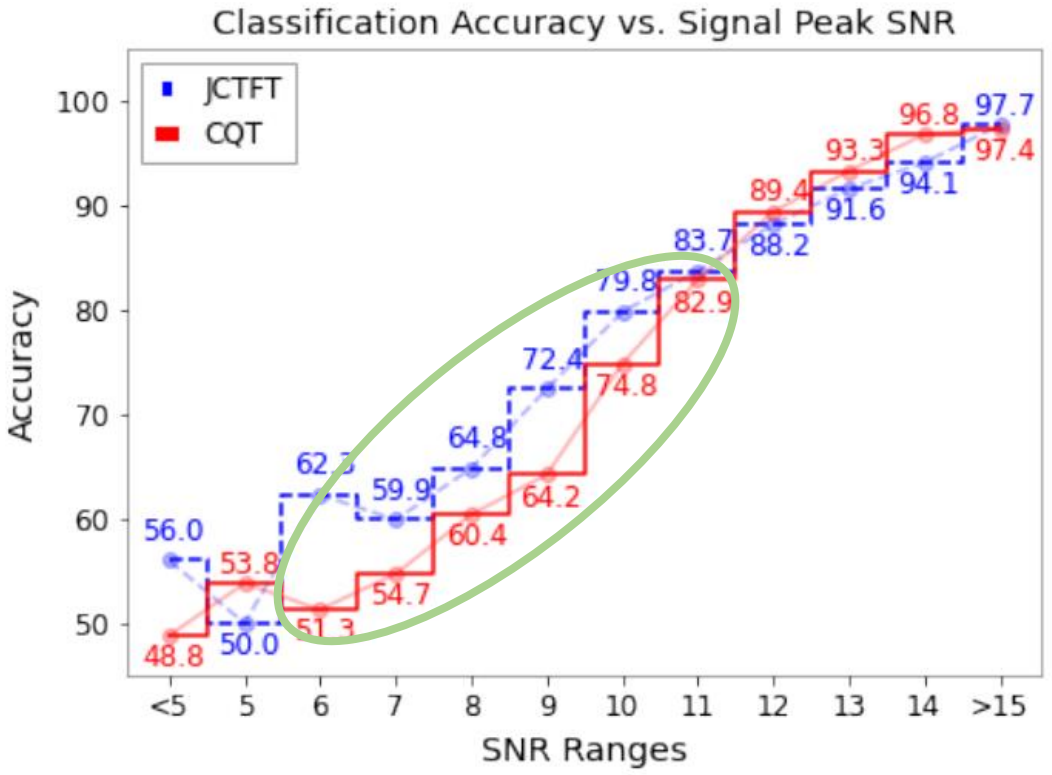

*SNR-categorized **classification accuracy** of the JCTFT and QT-trained Inception merger detection network.*

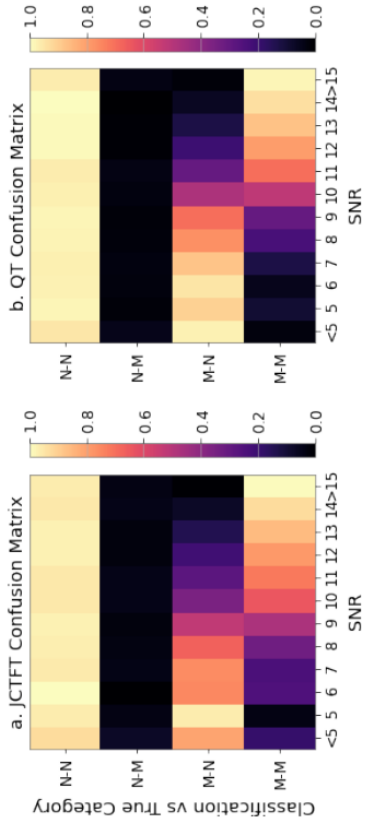

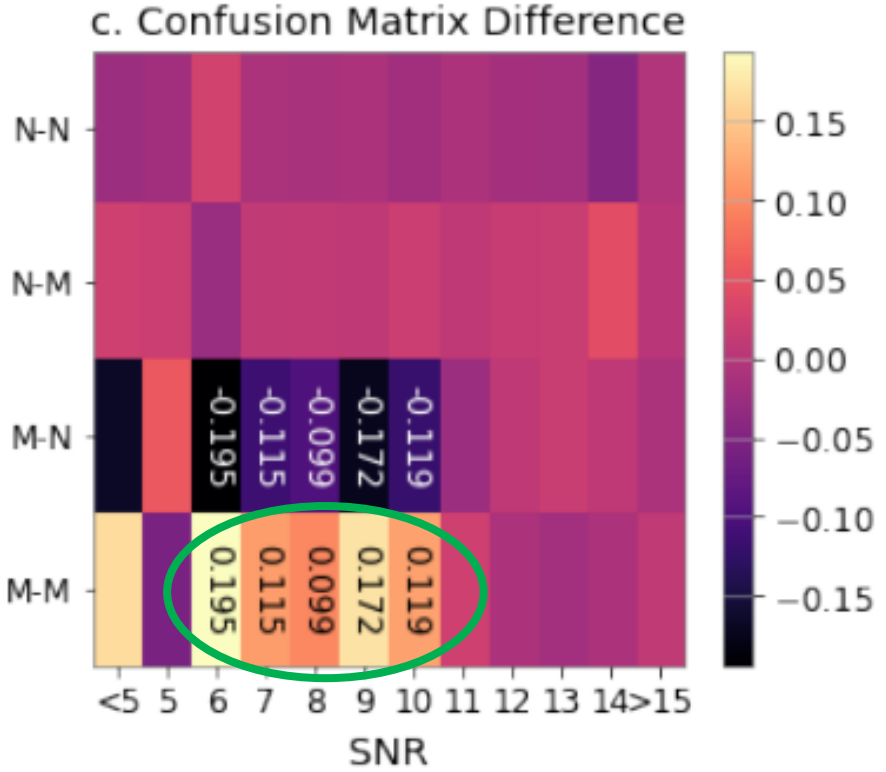

*SNR-categorized **confusion matrix** of the JCTFT and QT-trained Inception merger detection network.*

*On average **14% higher merger-merger accuracy** for simulated BBH merger signals with SNR 6-10.

Conclusions and Future Work

Conclusions:

- The JCTFT decomposes time-series signals into chirp rate, time and frequency, and establishes the relationship between the three quantities.
- Improved neural network classification accuracy using simulated BBH merger signals with SNR 6-10.
- The JCTFT and methods extended from it pave the way for new three-dimensional chirp signal search and analysis techniques, using either classical methods or machine learning algorithms.

Conclusions and Future Work

Next,

- An improved chirp signal peak detection algorithm for more accurate chirp-rate estimation.
- Probe the potential of detector glitch classification and analysis using the JCTFT.
- Investigate the JCTFT periodicity and signal peak characteristics.
- Investigate the effects of these methods in low-latency ANN BBH merger detection pipelines.

- Potential applications in radar, lidar, sonar, and geophysical data analysis?
  (Since this is a session focused on nuclear and particle theory, do you experts see applications of the JCTFT in data analysis in your fields?!)

Visiting PhD candidates:

- Developing Data Analysis Techniques for Gravitational Wave Detectors – ***Xuehao Zhang (Lanzhou University)*** – 2 years

- Search Methods for Deterministic Gravitational Wave Sources and Their Application to Pulsar Timing Arrays – ***Yiqian Qian (Huazhong University of Science and Technology)*** – 1 year

  In collaboration with Professor Soumya Mohanty at the University of Texas Rio Grande Valley (UTRGV)

Mitacs Undergraduate Exchange Students:

- Pulsar Spin-down Coefficients - Varenya Upadhyaya 2023
- Lambert W Function - Soumya Kanti Saha 2023
- Neural Networks and GW Detection - Jignesh Mohanty 2022
- ….

Western UNIVERSITY · CANADA

The University of Texas Rio Grande Valley

Mitacs

Contacts:
Prof. Sree Ram Valluri: valluri@uwo.ca

Xiyuan Li: xli2522@uwo.ca

Parameter	Value	Parameter	Value
Input Sample Frequency (s^{-1})	2048	γ^* (s^{-2})	0 - 2400
JCTFT Sample Frequency (s^{-1})	600	C^* (s^{-2})	60
Ω (s^{-1})	30 - 300	l^*	0 - 40
Ω_0^* (s^{-1})	25	$\sigma^*(s^{-1})$	6
μ^*	0.0075		

Table 1: JCTFT parameter values or ranges used for generating the results in this paper unless specified otherwise. The JCTFT sampling frequency and Ω are determined based on detector specifications [34]. Parameters labeled by * are estimated based on determined values using equations (1), (6), and (9). Different combinations may produce better or worse results.

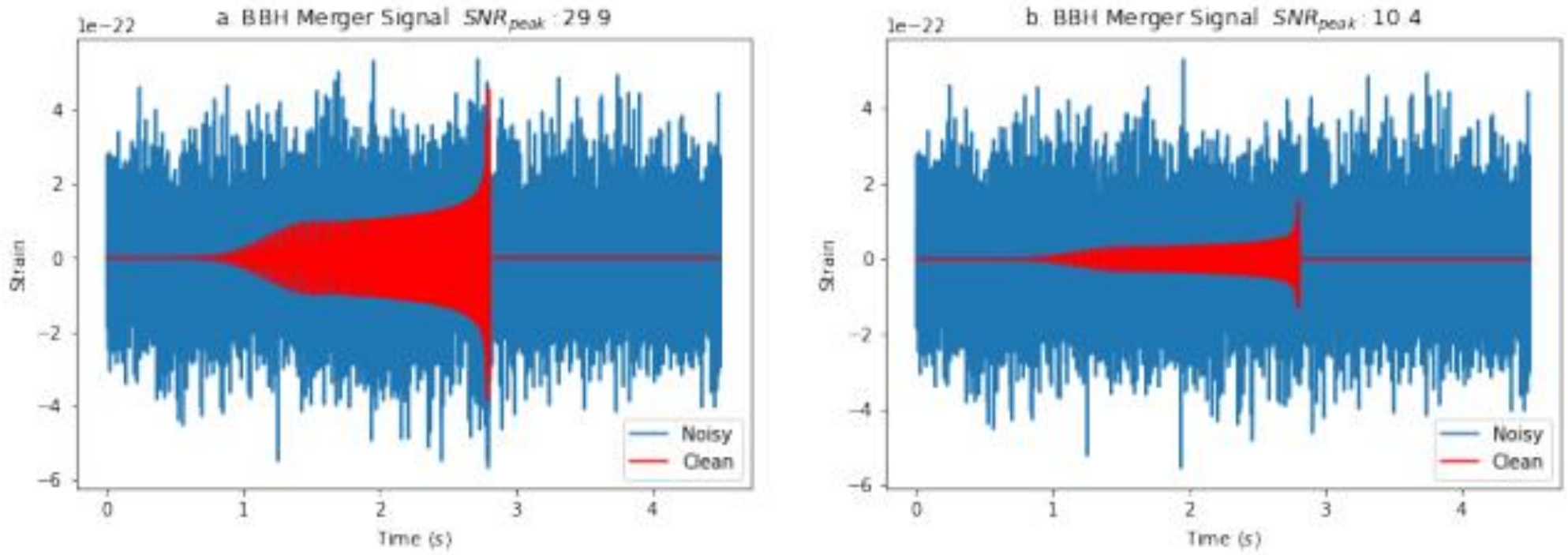

Figure 3: (a) Signal $h^{29.9}_{SNR}(t)$: Simulated high SNR BBH merger GW signal strain $h^{600}_{Mpc}(t)$ with aLIGO detector characteristic noise. (b) Signal $h^{10.4}_{SNR}(t)$: Simulated low SNR BBH merger GW signal strain $h^{1800}_{Mpc}(t)$ with aLIGO detector characteristic noise. Noisy signals $h^{29.9}_{SNR}(t)$ and $h^{10.4}_{SNR}(t)$ are plotted in blue. Merger signals are plotted in red.

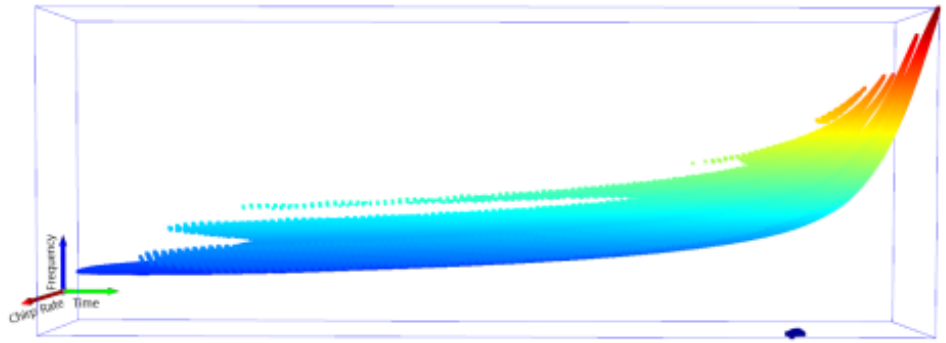

Figure 4: Processed JCTFT result of merger signal $h^{600}_{Mpc}(t)$ plotted in three-dimensional space. The green, blue, and red axes indicate time, frequency, and chirp rate. Red voxels represent higher frequencies, and blue voxels represent lower frequencies.

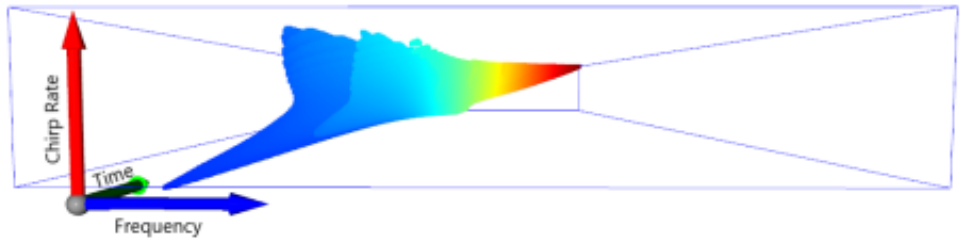

Figure 5: Processed JCTFT result of merger signal $h^{600}_{Mpc}(t)$ plotted in three-dimensional space. The green, blue, and red axes indicate time, frequency, and chirp rate. Red voxels represent higher frequencies, and blue voxels represent lower frequencies.

Appendix

Parameters	Values
Sample Frequency (s^{-1})	2048
Lower-Frequency Cut-off (s^{-1})	30
Spectrogram Shape (pixels)	256*256*3
Combined Pre-merger Mass ($M_{\odot}$)	10 - 83
Distances (kMpc)	0.6 - 1.2
	1.4 - 2
Z-axis Spin	[-1,1]
Spin Beta Distribution	$\alpha = \beta = 0.125$
Merger Position (s)	2, 3, or 4 $\pm$ 0.5
	Normal Distribution

Table A1: Training and Testing Dataset Parameter Values.

M1200 contains 12,500 simulated noisy merger waveforms from BBH systems between 600 Mpc and 1200 Mpc, and 12,500 aLIGO detector noise waveforms; M2000 contains 12,500 simulated noisy merger waveforms from systems between 1400 Mpc and 2000 Mpc, and 12,500 aLIGO detector noise waveforms. The merger waveforms were simulated for systems with combined pre-merger masses between 10M⊙ and 83M⊙.

Appendix